Arch. Metall. Mater. **69** (2024), 2, 613-623

DOI: https://doi.org/10.24425/amm.2024.149790

S.M. MUTHU[1], M. ARIVARASU[2*], K. JITHESH[3], M. VIGNESH[4],
V. DHINAKARAN[1], P. SURESH KUMAR[5]

HOT CORROSION STUDIES ON HVOF COATED ALLOY A-286 IN MOLTEN SALT ENVIRONMENT

The corrosion resistance Cr_3C_2-25%NiCr and Ni-20%Cr coatings were deposited on the alloy A-286 by high-velocity oxy-fuel (HVOF) coating, and the high-temperature corrosion features were evaluated at 700 and 850°C in Na_2SO_4-5%NaCl-7.5%$NaVO_3$ atmosphere. Deposited coatings are dense and well-adherent to the substrate. A scanning electron microscope (SEM) is used to analyze the structure of the corroded samples. Results showed that Cr_3C_2-25%NiCr coating provides better resistance to corrosion at 700°C, which is attributed to the protective Cr_2O_3 development. The coated metal was exposed at 850°C, and a higher corrosion rate was observed compared to 700°C, indicating that the temperature influenced the oxidation rate. The coating failure (crack) was noticed on the Cr_3C_2-25%NiCr coated surface when exposed at 850°C, and no damages are in the Ni-20%Cr coating.

Keywords: Alloy A-286; High-velocity oxy-fuel coating; High temperature corrosion; Corrosion kinetics; Morphology

1. Introduction

Fe-based alloy A-286 is extensively used as a structural material in marine, aircraft, and gas turbine engine components due to their excellent oxidation resistance and creep-rupture strength at elevated temperatures. Hot corrosion is a major problem in the aforementioned areas, where the alloy comes in contact with various kinds of fuels, such as fossil fuels and low-grade fuel oils, at high temperatures. This alloy has lower thermal expansion at high temperatures than the Ni and Co-based superalloys. The materials working at elevated temperatures in the air and the corrosive environment get oxidized and form an oxide layer which may be protective or non-protective [1-3]. Sodium from the air and the presence of sulfur and vanadium in fuel will turn into intricate molten salt compounds such as Na_2SO_4, $NaVO_3$, V_2O_5, and NaCl during combustion. At high temperatures, these salts and surrounding O may cause alloy components to degrade, reducing service life. The gas turbine and marine engine components were susceptible to sulphidation and oxidation in sulfate salt medium. The fluxing (namely acidic and basic fluxing) is the series issue in hot corrosion that occurs by the reaction of oxides and molten salt. Along with Na_2SO_4, NaCl also plays a crucial role that could destroy the protective layers. Alloy is prone to corrosion attack in the salt atmosphere due to developing a loose and porous Fe_2O_3 layer [4-6].

Thermal spray coating techniques are extensively used for the application of erosion and corrosion resistance in gas turbines, boilers in steam power plants, and waste heat incinerators to protect the material from aggressive gas and salt environments at high temperatures. Ceramics as a coating material could significantly enhance the properties due to the high hardness, strength, low thermal conductivity, and high thermal stability of the coated oxides [7-8]. This research has focused primarily on increasing the service life of components by improving the surface properties of alloy components. The capability to resist the environmental impact is the most important consideration in choosing a protective coating for usage at elevated temperatures, but other aspects such as base material, application, applied load on component, design of the component, and so on play vital roles. Thermal spray metal-ceramic coating is an effective technique; it offers better corrosion resistance and mechanical properties to the various metallic components [8-9]. Various thermal spraying techniques such as high-velocity oxy-fuel (HVOF), detonation gun, cold spray, and plasma spray are widely em-

[1] CHENNAI INSTITUTE OF TECHNOLOGY, CENTRE FOR ADDITIVE MANUFACTURING, CHENNAI-600 069, INDIA
[2] VELLORE INSTITUTE OF TECHNOLOGY, CENTRE FOR INNOVATIVE MANUFACTURING RESEARCH, VELLORE-632 014, INDIA
[3] ADI SHANKARA INSTITUTE OF ENGINEERING AND TECHNOLOGY KALADY, DEPARTMENT OF MECHANICAL ENGINEERING, INDIA
[4] VELLORE INSTITUTE OF TECHNOLOGY, SCHOOL OF MECHANICAL ENGINEERING, VELLORE-632014, INDIA
[5] RAMCO INSTITUTE OF TECHNOLOGY, DEPARTMENT OF MECHANICAL ENGINEERING, RAJAPALAYAM, INDIA

* Corresponding author: arivarasu.m@vit.ac.in; arivarasu.m@gmail.com

ployed for depositing hard metallic coatings. Out of these, high-velocity oxy-fuel (HVOF) coating is one of the ideal techniques for depositing metallic, cermet, and carbide-based coating on the components exposed to high-temperature corrosion, erosion, and wear conditions. In this coating technique, a mixture of two or more powders and wire-formed coating materials is melted fully or partially and injected uniformly at high velocity over the substrate surface. As a result, HVOF coatings can achieve good substrate adhesion, low porosity, high hardness, and more dense coating characteristics. Furthermore, HVOF coating can be able to deposit thicker coating in energy sectors for corrosive and erosive resistance compared to hard chromium plating, physical vapour deposition (PVD), and chemical vapour deposition (CVD) [10-14]. The selection of an appropriate coating material for a specific application necessitates the knowledge of a particular service environment and the chemical composition of the substrate material. Deposition of nickel-chromium-based coating is a cost-effective approach to improving the tribological performance of surfaces exposed to an aggressive environment. Nickel provides strength in the coating, while chromium protects the components against hot corrosion. Several researchers have developed the Cr_3C_2-25%NiCr coating for corrosion, erosion, and wear-resistant applications due to its high hardness, melting point, and strength. As a result of the combination, the substrate's corrosion resistance and wear properties are improved [14-16].

Sidhu et al. [7] compared the corrosion resistance between bare metal (superni 75, superni 601) and material coated with Cr_3C_2-NiCr coated sample under an aggressive Na_2SO_4-60%V_2O_5 medium in cyclic conditions (900°C). The experimental results proved that the samples coated with Cr_3C_2-NiCr showed better corrosion resistance when compared to bare metal. It reduces weight gain by 70%. Sidhu et al. [10] deposited Ni-Cr wire on the Fe and Ni-based superalloys for hot corrosion resistance applications using the HVOF method. Further, the microstructural and mechanical properties of the coatings were characterized. Satish et al. [11] used the HVOF method to deposit Molybdenum wire on the low-carbon steel to enhance the wear behavior. Senderowski et al. [12] conducted hot corrosion studies on low-carbon steel (AISI 4135) deposited with various compositions of Fe-Al powders by the HVOF coating technique. The performance of deposited coatings subjected to Na_2SO_4 at 850°C was evaluated by cross-sectional analysis for the diffusion of the corrosive elements Na and S. Senderowski et al. [13] deposited Ni-Cr and Ni-Al interlayer on the 1045 steel using gas detonation spray method, and further Fe-Al coating was deposited on the interlayer. The authors studied the influence of the structure, hardness, and thermal stability of the Fe-Al coating on the interlayer. Bala et al., [17] studied the oxidation performance of the Ni-20Cr and Ni-50Cr coatings employed by the cold-spray method on SAE 213 steel under cyclic heating (900°C). It was reported that the bare steel was prone to spalling and sputtering. The results stated that the coated samples were more resistant to oxidation under superheated conditions when compared to the bare metal.

No reported works are available to improve the corrosion behavior of the alloy A-286 by the HVOF method in a turbine environment at two different temperatures. This work aims to examine the corrosion characteristics of the Cr_3C_2-25%NiCr and Ni-20%Cr coated alloy A-286 by HVOF at 700 and 850°C. Phase analysis was performed on the corroded samples using X-ray diffraction (XRD). The cross-sectional analysis was conducted on the corroded samples to evaluate the layer formation and corrosive species distribution using SEM and EDS mapping analysis.

2. Experimental work

2.1. Substrate material

A plate form of 4 mm thick Fe-based alloy A-286 was chosen as a substrate, and the composition of the alloy was examined by the optical emission spectroscopy method and reported in TABLE 1. Prior to the hot corrosion experiment, four specimens were cut from the plate with dimensions of 20 × 10 mm. Standard metallographic methods were used to polish each specimen using SiC grit papers of various sizes and were cleaned using acetone, followed by hot air drying to remove moisture content.

2.2. Coating deposition

To improve the coating adhesion, the six sides of the specimens were grounded with SiC sheets, followed by grit blasting using alumina particles. Two types of coating powders, Cr_3C_2-25%NiCr and Ni-20%Cr, were chosen for comparative study, considering their resistance to the high-temperature corrosion environment of Na_2SO_4-7.5% $NaVO_3$-5% NaCl. Before coating deposition, the samples were manually polished with SiC sheets to remove the oxides and other contaminants and then grit blasting with alumina particles to produce a rough surface which could enhance the adhesive strength of the coating with the substrate. Then the samples were cleaned with water and acetone ultrasonically. The HVOF coating technique was used to deposit Cr_3C_2-25%NiCr and Ni-20%Cr powders on the samples using Metco DJH 2603 gun at spraymet coating surface technologies, Bangalore. The HVOF coating process parameters are listed in TABLE 2.

TABLE 1

Chemical composition of the alloy A-286

Alloy	C	Mn	Si	Co	Cr	Ni	Mo	Ti	Al	Cu	V	Fe
A-286	0.046	1.21	0.505	0.32	13.6	24.1	1.18	1.99	0.25	0.298	0.15	56.2

TABLE 2

Process parameters for the HVOF process

Parameters	Values	Units
Oxygen pressure	1.13	MPa
Oxygen flow rate	13	lpm
Hydrogen pressure	0.735	MPa
Hydrogen flow rate	26	lpm
Powder feed rate	60	g/min
Powder particle size	40-60	µm
Spray distance	230	mm

2.3. Hot corrosion study

The hot corrosion studies were done on the Cr_3C_2-25%NiCr, and Ni-20%Cr coated specimens for 50 cycles at 700 and 850°C. Four specimens are properly weighed, and their physical dimensions are documented. A salt mixture of Na_2SO_4-7.5%$NaVO_3$-5%NaCl was applied on the six sides of the surface of the sample to simulate a turbine environment. The salt coating (3-5 mg/cm^2) was done manually using a wire brush. During salt deposition, samples were heated in an oven at around 250°C to support good adherence of the salt mixture on the samples. Individual alumina boats were employed to make it easier to handle the specimens. It was heated for 2 hours at 120°C in a box furnace to eliminate the moisture from the salt-applied specimens. Subsequently, the salt-coated specimens were kept inside the tubular furnaces with an alumina boat and the furnace temperature was increased by 5°C/min to 700 and 850°C for hot corrosion study. Each cycle consists of one-hour heating followed by 20 min cooling at atmospheric room temperature. At the end of each cycle, weight changes were evaluated using an electronic weighing balance (accuracy 0.0001 g) and documented. Also, the macro images were taken for visual examination.

The corroded samples were subjected to slicing for the cross-sectional analysis using diamond saw cutter. The surface morphology of coated and bare specimens was analyzed by scanning electron microscopy and energy dispersive spectroscopy (EDS) made by Carl Zeiss EVO/18. XRD analysis was conducted using Bruker D8 advance to identify various phases presented in the corroded samples.

3. Results

3.1. Visual analysis

Photographs of the Cr_3C_2-25%NiCr and Ni-20%Cr coated an alloy A-286 after corrosion in the molten salt conditions at 700, and 850°C are depicted in Fig. 1. It is noticed from the macro images at 700°C, the green color patches were present in the scales formed on the specimen, this suggests that the deposited molten salts. The specimen's color was changed to dark black during exposure to the salt atmosphere. Corroded specimens at 850°C, color was turned to dark black with grey, indicating that the oxide scales formation [8,14,15]. Due to thermal stress,

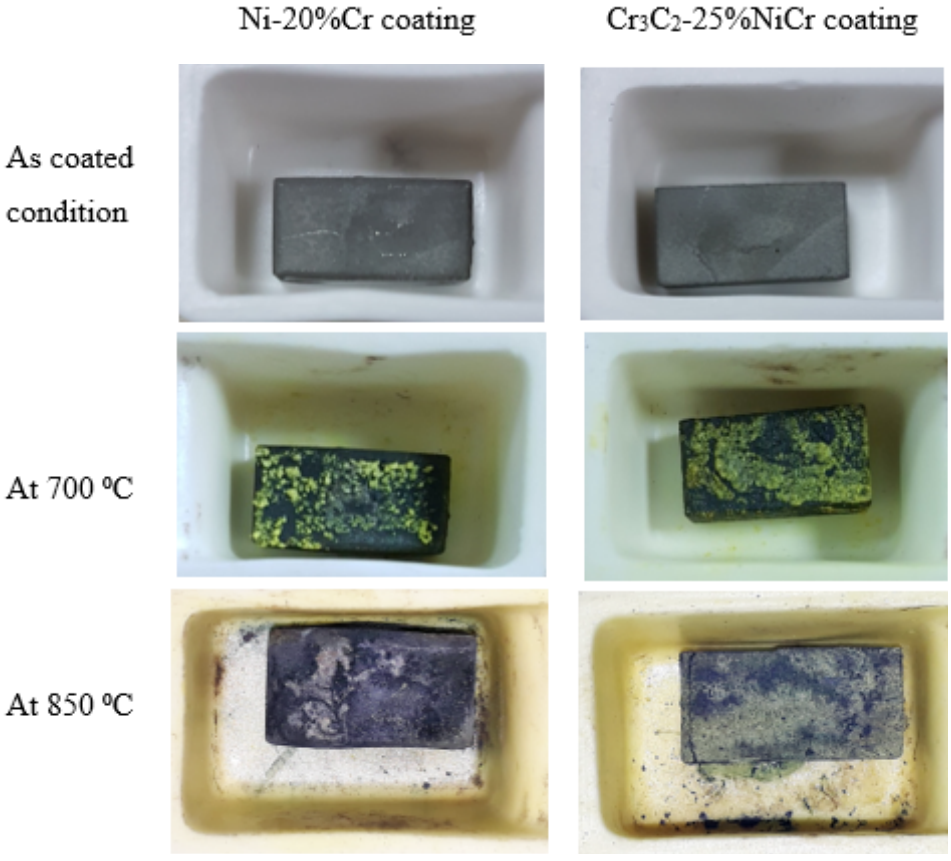

Fig. 1. Macro-images of the HVOF sprayed alloy A-286 during hot corrosion at 700°C after 50 cycles

cracks appeared on the corner of the Cr3C2-25%NiCr coated specimen at the 22nd cycle. A minor oxide scale spallation was noticed after 50 cycles of the corrosion study due to the development of protective, homogenous, and dense scales. The spalled scales were retained in the crucible and included during the weight measurement.

3.2. Thermogravimetric analysis

The weight gain plots for the HVOF sprayed specimens after hot corrosion at 700, and 850°C are represented in Fig. 2. As can be inferred from the weight gain plot, higher weight gain is observed at 850°C as compared to 700°C in both the coatings. Less weight gain is found in Cr_3C_2-25%NiCr coated specimen at both temperatures. Corrosion specimen coated with Ni-20%Cr at 850°C shows high weight gain, and rapid weight gain is witnessed till the end of the exposure.

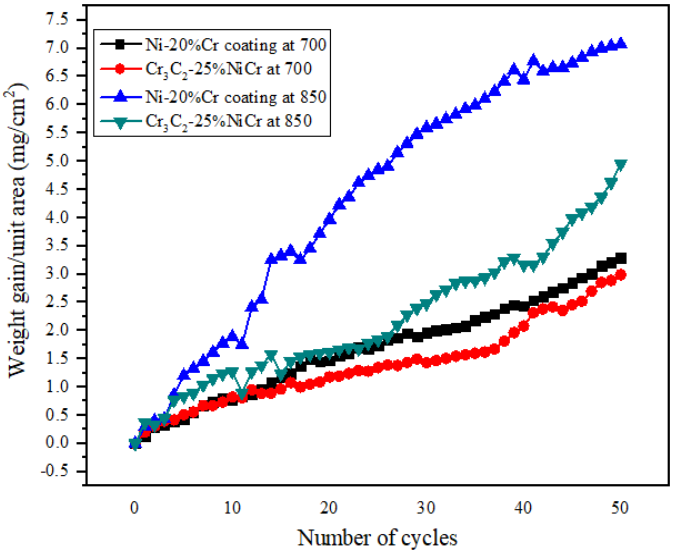

Fig. 2. Thermo-gravimetric analysis of the hot corroded HVOF sprayed alloy A-286 specimens after hot corrosion

In both the case of temperatures, the Kp values for Cr_3C_2-25%NiCr coating are significantly lower than the Ni-20%Cr coating. The cumulative weight gain along with parabolic constant (Kp) values of the coated specimens after exposure are listed in the TABLE 3.

TABLE 3

Weight gain and parabolic rate constant (Kp) of the coated A-286 alloy after corrosion at 700 and 850°C

	Weight gain ($mg \cdot cm^{-2}$)		Parabolic rate constant (Kp) ($\times 10^{-10}\ g^2 \cdot cm^{-4} \cdot s^{-1}$)	
Coatings/ Temperature	700°C	850°C	700°C	850°C
Ni-20%Cr	3.291	7.071	0.602	2.777
Cr_3C_2-25%NiCr	2.989	4.956	0.496	1.574

3.3. XRD analysis

XRD analysis for the scales formed on the HVOF sprayed alloy A-286 specimens after hot corrosion is depicted in Figs. 3 and 4. In the case of Ni-20%Cr coated specimens, NiO is the predominant phase, whereas Cr_2O_3 is the main phase in Cr_3C_2-25%NiCr coated specimens. In both the case of coatings, common oxide phases NiO, Cr_2O_3, $NiCr_2O_4$, NiS, CrS, and $NiVO_3$ were found.

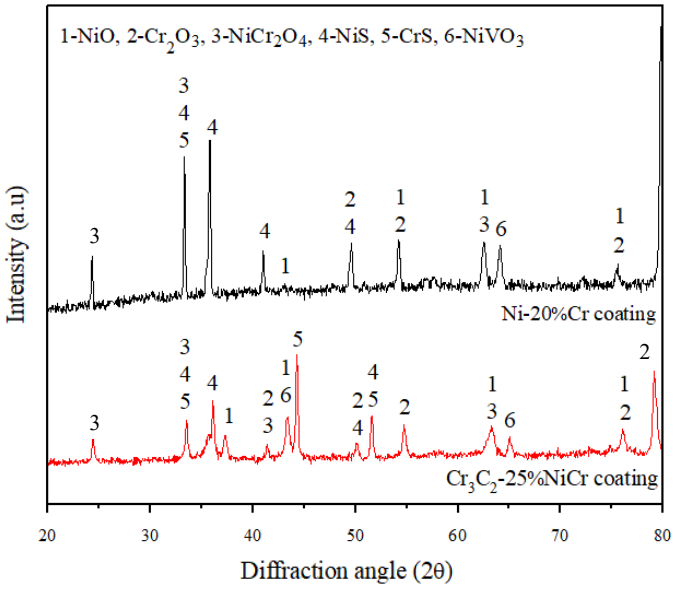

Fig. 3. XRD results of coated alloy A-286 after corrosion at 700°C

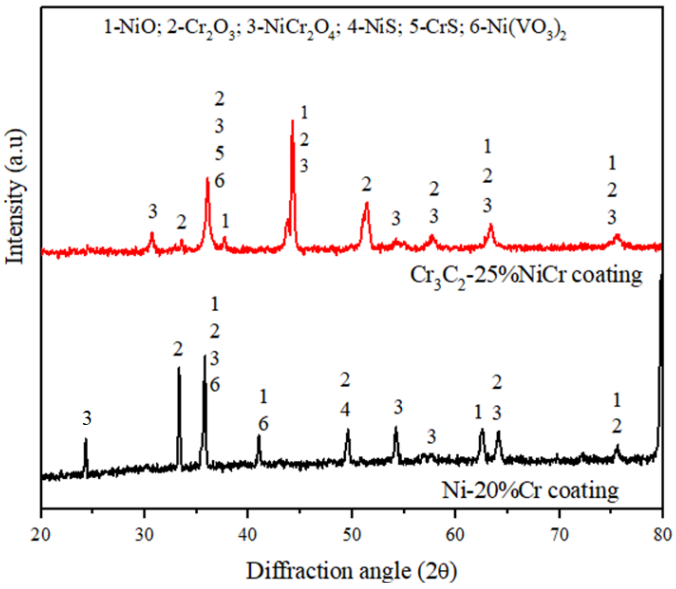

Fig. 4. XRD results of coated alloy A-286 after corrosion at 850°C

3.4. SEM/EDS analysis

The SEM microstructure study is performed on the HVOF coating on alloy A-286 after the corrosion study of 50 cycles. The oxides formed on the Ni-20%Cr and Cr_3C_2-25%NiCr coated

specimens after corrosion at 700°C (Fig. 5) show the flake-like morphology. The EDS analysis results indicate that the scales developed on the Ni-20%Cr coating are rich in Ni, O, and Cr, along with a minor amount of V, Na, and S. Cr, O and Ni are the main elements in the scales on the Cr_3C_2-25%NiCr coating, this suggesting that the formation of NiO and Cr_2O_3.

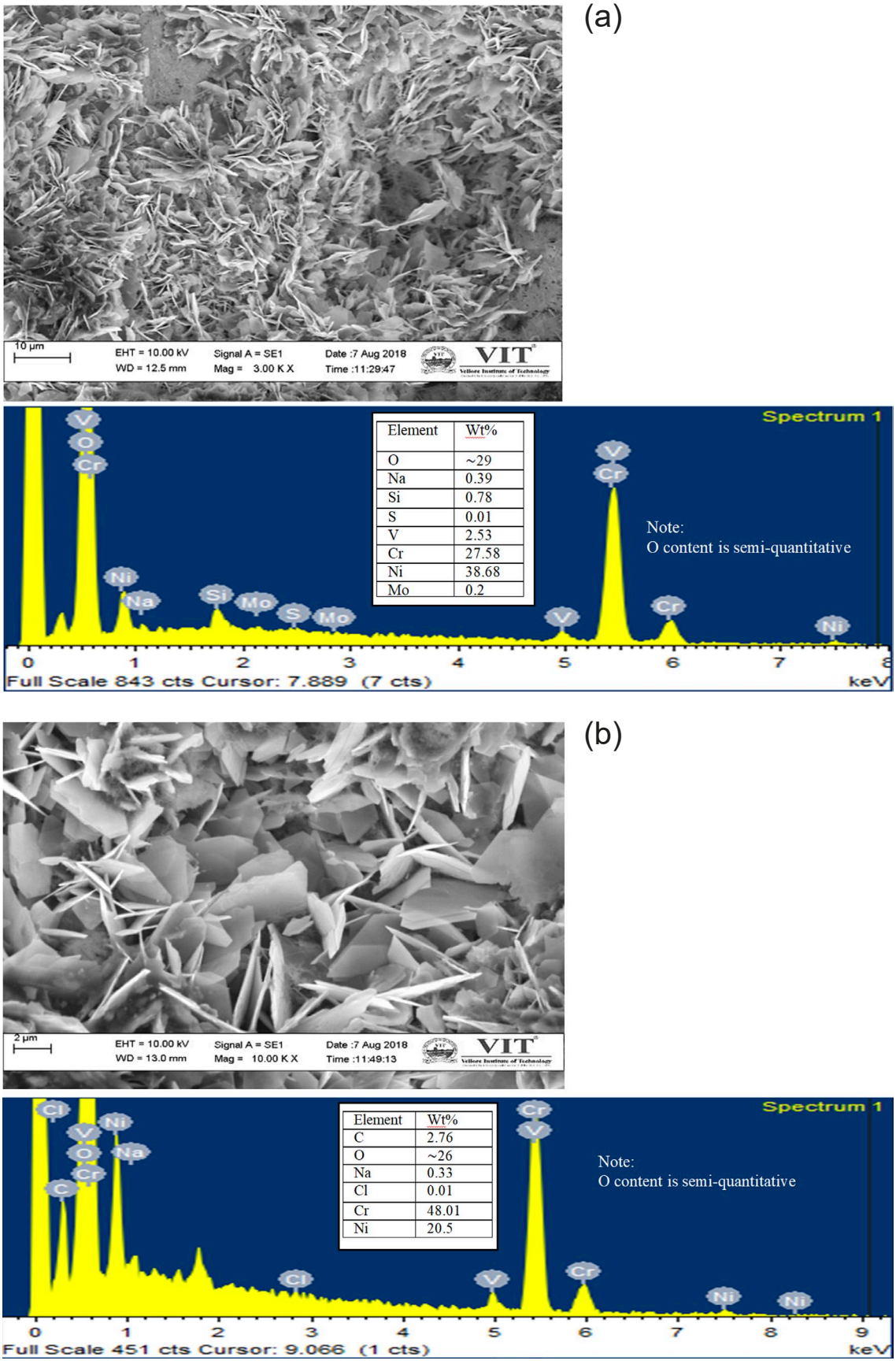

Fig. 5. SEM/EDS analysis of the HVOF (a) Ni-20%Cr and (b) Cr_3C_2-25%NiCr coated specimen alloy A-286 after exposure to molten salt at700°C

Fig. 6 represents the SEM micrograph of the HVOF sprayed alloy A-286 after being exposed to the corrosion environment at 850°C. The scales on the Ni-20%Cr coated specimen (Fig. 6(a)) show the rod and plate-like morphology and consist of O, Ni, and Cr which is confirmed by EDS results. In the scale of corroded Cr_3C_2-25%NiCr coated specimen (Fig. 6(b)), a flake-like

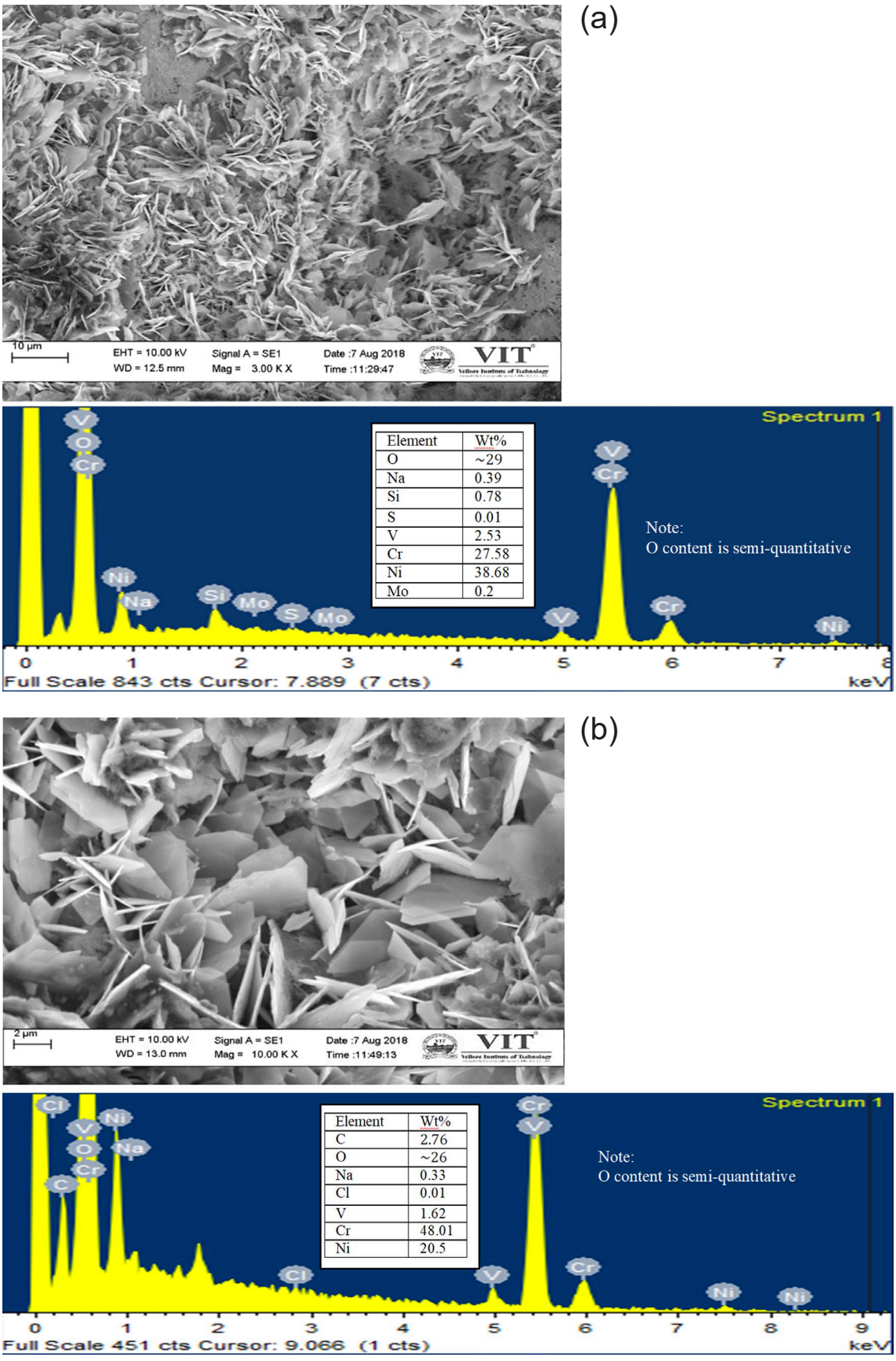

Fig. 6. SEM/EDS analysis of the HVOF (a) Ni-20%Cr and (b) Cr_3C_2-25%NiCr coated specimen alloy A-286 after exposure to molten salt at 850°C

microstructure was found, mainly rich in O, Cr and Ni. A minor Fe is noticed in the scale, suggesting diffusion from substrate. The presence of corrosive species such as Na, Cl, V, and S are smaller in both coated specimens.

3.5. Cross-sectional analysis

SEM cross-sectional micrograph of the Ni-20%Cr and Cr_3C_2-25%NiCr coatings on the alloy A-286 after corrosion at 700 and 850°C is described in Figs. 7-10. In the case of both temperature, a very thin layer of scale appeared on the Ni-20%Cr coated specimen at the top surface, and the thickness of the scales were observed in the range of 8-10 µm and 10-15 µm 700 and 850°C. The EDS results show that the scales mainly consist of O, Ni, and Cr. This confirms the development of NiO and Cr_2O_3 scales which gives the necessary protection to the substrate material, and no corrosion products are found in the substrate. Other corrosive elements such as Na, S, V, and Cl are distributed partially in the coating region.

SEM micrograph illustrates a thin oxide layer on the Cr_3C_2-25%NiCr coated specimens in both the temperatures and the scale thicknesses found in the range of 8-10 µm and 10-12 µm 700 and 850°C. There is no corrosion attack is found in the substrate. Results of elemental mapping analysis clearly show the existence of O, Cr and Ni in the top region and the coating region mainly contain the high amount of Cr and Ni with the minor amount of Na, S, Cl and V are partially present in the coating region which is not found in the substrate zone. It is inferred from the cross-sectional analysis; both the coatings act as a diffusion barrier to the substrate material and enhance the corrosion resistance at both the temperatures due to the formation of protective Cr_2O_3, $NiCr_2O_4$ and NiO scales.

4. Discussion

The corrosion resistance coatings were deposited using the HVOF method on the Alloy A-286. The corrosion studies were conducted on the coated samples in Na_2SO_4-7.5%$NaVO_3$-5%NaCl medium at 700 and 850°C. The coatings are oxidized when exposed at elevated temperature in the presence of corrosive salt and air during cooling. New scales were developed on the coating during the exposure due to the reaction of Ni, Cr elements with air according to Eqs. 1-3 and as a result change in color was observed [17-20]. The scales fully cover the entire surface of the coating. Less weight gain was noticed at 700°C as compared to 850°C. This indicates that the temperature influences the corrosion behavior of the coating. In the Ni-20%Cr coating, NiO, $NiCr_2O_4$, and Cr_2O_3 are the predominant scale

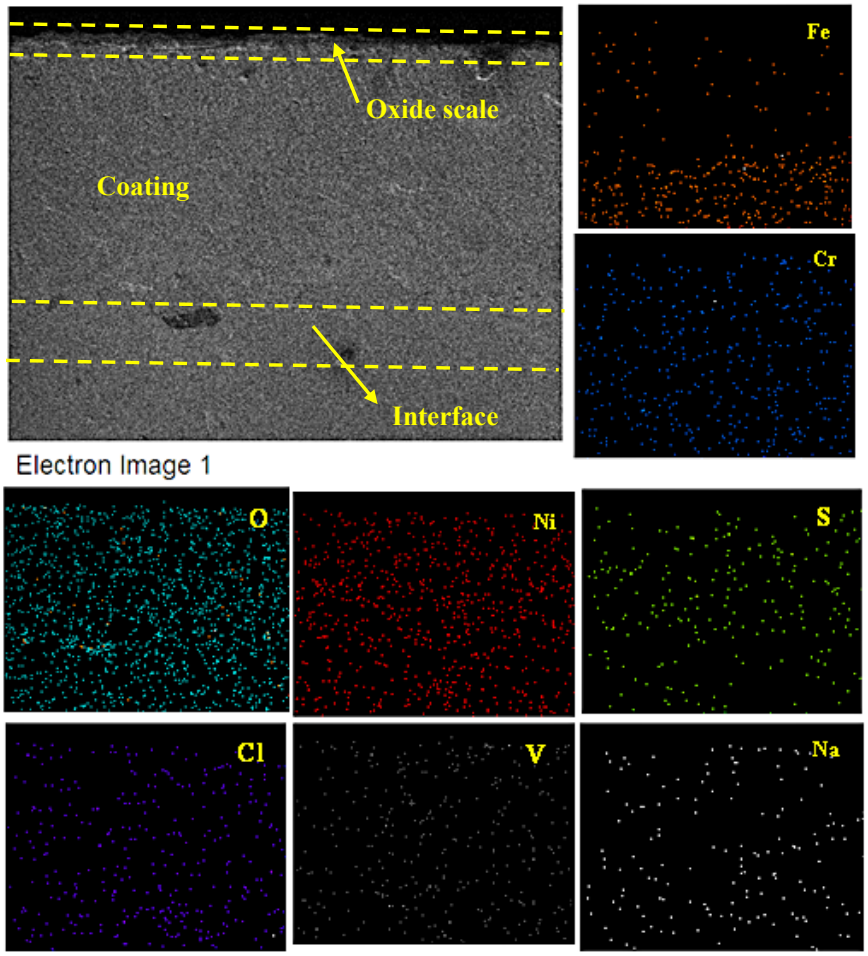

Fig. 7. SEM cross-sectional micrograph and elemental mapping analysis for the hot corroded Ni-20%Cr coated alloy A-286 at 700°C

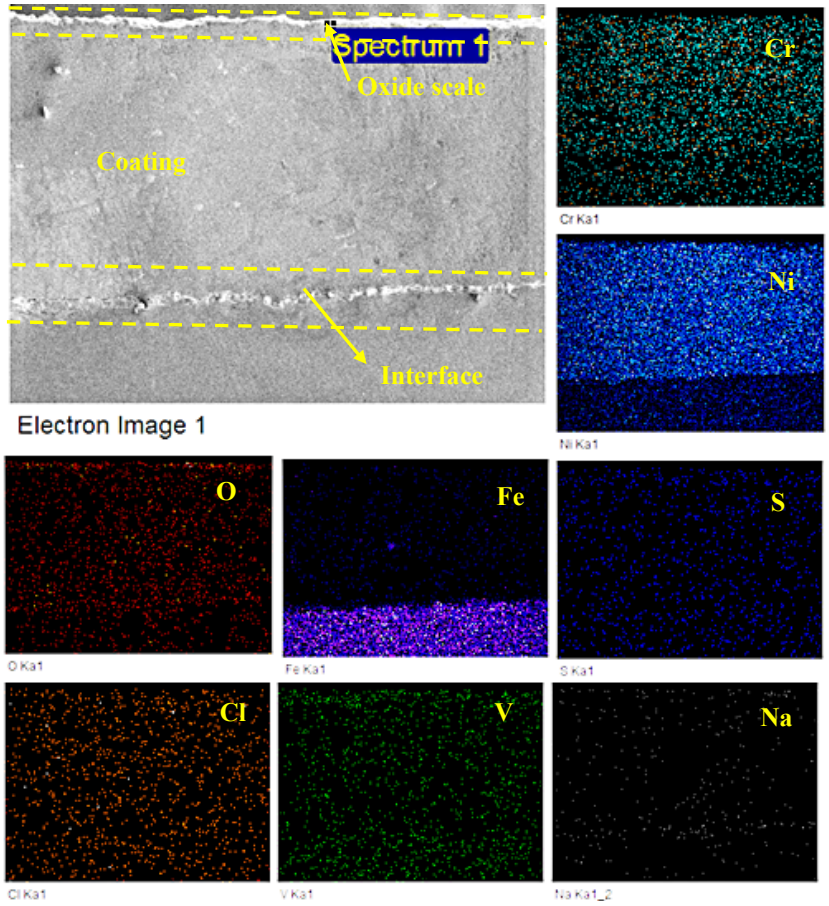

Fig. 8. SEM cross-sectional micrograph and elemental mapping analysis for the hot corroded Ni-20%Cr coated alloy A-286 at 850°C

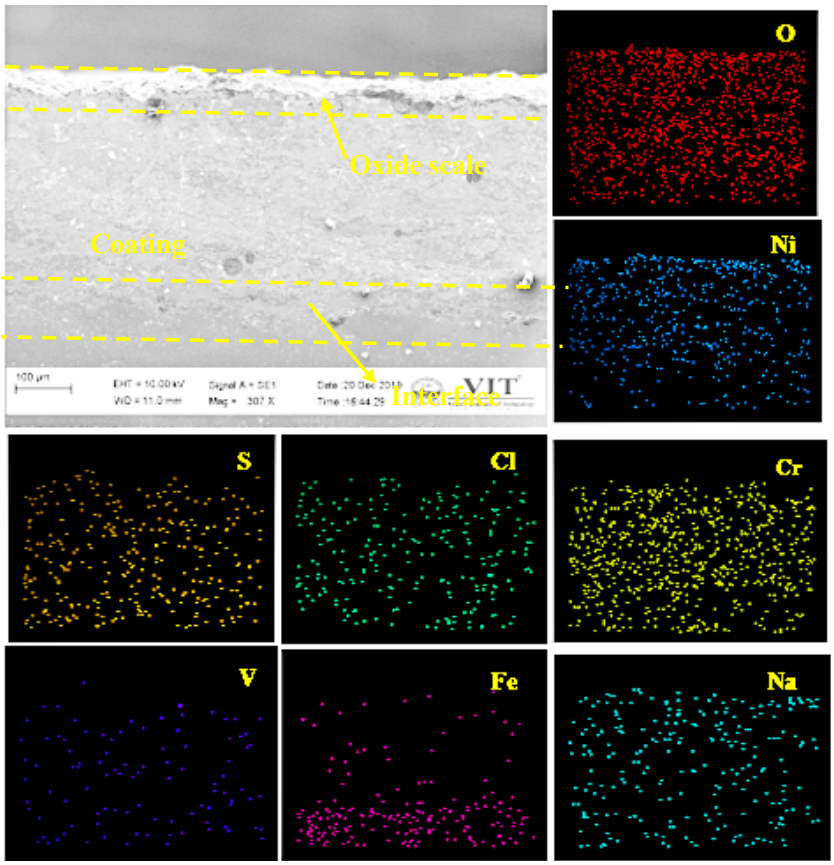

Fig. 9. SEM cross-sectional micrograph and elemental mapping analysis for the hot corroded Cr_3C_2-25%NiCr coated alloy A-286 at 700°C

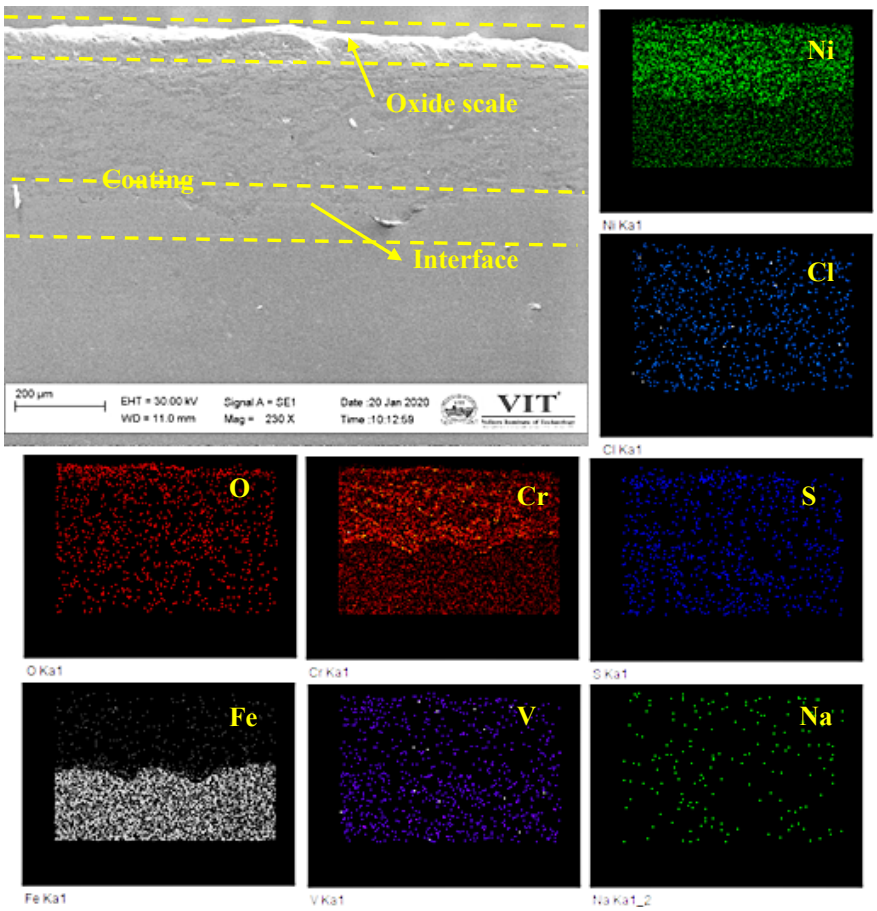

Fig. 10. SEM cross-sectional micrograph and elemental mapping analysis for the hot corroded Cr_3C_2-25%NiCr coated alloy A-286 at 850°C

which is confirmed by XRD and EDS results. No significant failures such as cracks and spallation were noticed on the coating when exposed at 700°C. Other corrosive species NiS, Cr_2S_3, and $NiVO_3$ are noticed. XRD detects no chlorides on the oxide scale surface.

$$Ni + O \rightarrow NiO \quad (1)$$

$$2Cr + \frac{3}{2}O_2 \rightarrow Cr_2O_3 \quad (2)$$

$$NiO + Cr_2O_3 \rightarrow NiCr_2O_4 \quad (3)$$

Linear weight gain was observed in both the case of coatings at 700°C, indicating the continuous oxidation in the presence of the corrosive salt. The corrosion kinetic plot involves the growth of the oxides, dissolution of reaction products, and exfoliation. Anti-corrosive element (Cr) in the coatings could affect the oxides growth by forming protective Cr_2O_3 (till 900°C) and avoiding salt penetration. Cr_2O_3 easily formed on the coating in the air condition due to higher affinity of Cr with O. However, a mixture of NiO and $NiCr_2O_4$ were present on the coating surface instead of continuous Cr_2O_3.

Na_2SO_4 does not melt at 700°C because of its high melting point (m.p 884°C). However, it combines with NaCl (m.p 800°C) and $NaVO_3$ (m.p 630°C) to form the low melting eutectic phase which could dissolve the scale. The melting point of eutectic mixture of salt is less than the test temperatures (700 and 850°C). Mannava et al. [21] performed the corrosion test on alloy 718 in the similar 3SM environment at 650°C. Due to Na^+ from Na_2SO_4 salt plays a crucial role in the degradation of scales formed on the coating. Na^+ could diffuse rapidly into the substrate due to the small iconic diameter. Na_2O reacts with Cr_2O_3 to form a Na-chromate at elevated temperature which could dissolve scales causing micropores and cracks were developed on the protective scales [21-23]. The salts once penetrated the coating through cracks, the coating would subject to severe corrosion attack. Moreover, S promotes the formation of metal sulfides which could detected by XRD.

The melted $NaVO_3$ (m.p 630°C) could diffuse into the coating through the pores in the scales and further increasing oxidation rate. In addition, vanadium promotes the growth rate of oxides causing continuous weight gain was noticed till the end of test. Mannava et al., [21] V_2O_5 reacts with NiO and Cr_2O_3 in the scales and forms $Ni_3V_2O_8$ and $CrVO_4$ according to Eqs. 4-5.

$$3NiO + V_2O_5 \rightarrow Ni_3V_2O_8 \quad (4)$$

$$Cr_2O_3 + V_2O_5 \rightarrow 2CrVO_4 \quad (5)$$

Furthermore, Na_2O reacts with Cr_2O_3 resulting in Na_2CrO4 and $Na_2Cr_2O_7$. The formed Na_2CrO_4 was noticed on the boat as yellow colour and $Na_2Cr_2O_7$ was evaporated as a gas reported by Rapp et al. [24]. XRD confirmed that no sodium dichromate

($Na_2Cr_2O_7$) in the scale and also literatures reported the absence of $Na_2Cr_2O_7$ above 400°C due to self-decomposition and evaporation of Na containing substance. The oxides were subjected to basic fluxing and corresponding to the following Eqs. 6-7.

$$Cr_2O_3 + Na_2O + \frac{1}{2}O_2 + O_2 \rightarrow Na_2Cr_2O_7 \quad (6)$$

$$NiO + O_2^- \rightarrow NiO_2^{2-} \quad (7)$$

Volatile chlorides were formed by the reaction of Ni, Cr elements in the coating with Cl suggesting that the coatings were subjected to chlorination and oxy-chlorination. Therefore, weight loss was noticed during the test. Some pits and pores were witnessed on the coating surface due to the existence of volatile species. EDS analysis reported that significant amount of O on the corroded coating surface, indicating the oxidation by the diffusion of air and other salt species through the pores formed by volatile species are described by Eqs. 8-11. XRD detected no metal chlorides on the corroded samples as a result of metal oxide and Cl formation due to oxidation and high vapor pressure promotes the metal chloride volatilization into the atmosphere [20,25].

$$Ni + Cl_2 \rightarrow NiCl_2 \quad (8)$$

$$Cr + Cl_2 \rightarrow CrCl_2 \quad (9)$$

$$NiCl_2 \rightarrow NiCl_2 \quad (10)$$

$$NiCl_2 + \frac{1}{2}O_2 \rightarrow NiO + Cl_2 \quad (11)$$

It can be concluded that Cr_3C_2-25%NiCr coating reduced the weight gain of the specimens than Ni-20%Cr coating at both temperatures. The coatings were severely susceptible to chlorination and sulphidation attack at 850°C causing coating cracks were found on the Cr_3C_2-25%NiCr. However, no corrosion attack was noticed on the substrate at 700 and 850°C.

5. Conclusions

The corrosion resistance coatings were successfully deposited on the alloy A-286 using the HVOF method, and the corrosion studies were done on the coated alloys at elevated temperatures. From the test results, the following conclusions were drawn.

1. The results indicate that more corrosion attack and weight gain was observed at 850°C, suggesting that the temperature influence the corrosion behaviour of the coating.
2. Cr_3C_2-25%NiCr coating improved corrosion resistance at 700°C due to the development of dense Cr_2O_3 scale and no coating failure was noticed.
3. Cracks were formed on the top surface of the Cr_3C_2-25%NiCr coating when exposed at 850°C due to more thermal stress. No cracks were found on the Ni-20%Cr coating.
4. NaCl leads to the formation of volatile chlorides, resulting in pits and pores appearing on the scales and $NaVO_3$ promotes the oxides growth rate.
5. Both the coatings exhibited the better protection to the substrate against corrosive salts due to the development of non-porous protective scales.

REFERENCES

[1] A.R. Salehi, S. Serajzadeh, N. Yazdipour, A study on flow behavior of A-286 superalloy during hot deformation. Mater. Chem. Phys. **101** (1), 153-157 (2007).
DOI: https://doi.org/10.1016/j.matchemphys.2006.03.012

[2] G. Shejale, R. Garg, G.V Subrahmanyam, A. Schnell, Condition Assessment Study of A-286 Alloy Gas Turbine Wheel. J. Fail. Anal. Prev. **16** (5), 712-717 (2016).
DOI: https://doi.org/10.1007/s11668-016-0154-6

[3] Y. Garip, Z. Garip, O. Ozdemir, Prediction modeling of Type-I hot corrosion performance of Ti–Al–Mo-X (X= Cr, Mn) alloys in $(Na, K)_2SO_4$ molten salt mixture environment at 900°C. J. Alloy Compd. **843**, 156010 (2020).
DOI: https://doi.org/10.1016/j.jallcom.2020.156010

[4] S.M. Muthu, D.A. Moganraj, Air Oxidation and Hot Corrosion Behavior of Bare and CO_2 Laser-Welded Superalloy A-286 at 700°C. Trans. Indian Inst. Met. **72** (2019).
DOI: https://doi.org/10.1007/s12666-019-01713-0

[5] Y. Garip, O. Ozdemir, Corrosion behavior of the resistance sintered TiAl based intermetallics induced by two different molten salt mixture. Corros. Sci. **174**, 108819 (2020).
DOI: https://doi.org/10.1016/j.corsci.2020.108819

[6] Y. Garip, An investigation on the corrosion performance of $Fe_2CoCrNi_{0.5}$ based high entropy alloys. Corros. Sci. **206**, 110497 (2022). DOI: https://doi.org/10.1016/j.corsci.2022.110497

[7] T.S. Sidhu, S. Prakash, R.D. Agrawal, Characterizations and hot corrosion resistance of Cr_3C_2-NiCr coating on Ni-base superalloys in an aggressive environment. J. Therm. Spray Technol. **15** (4), 811-816 (2006).
DOI: https://doi.org/10.1361/105996306X147162

[8] S.M. Muthu, A.M, Investigations of hot corrosion resistance of HVOF coated Fe based superalloy A-286 in simulated gas turbine environment. Eng. Fail. Anal. **107**, 104224 (2020).
DOI: https://doi.org/10.1016/j.engfailanal.2019.104224

[9] W. Zhou, K. Zhou, C. Deng, K. Zeng, Y. Li, Hot corrosion behaviour of HVOF-sprayed Cr_3C_2-NiCrMoNbAl coating. Surf. Coat. Technol. **309**, 849-859 (2017).
DOI: https://doi.org/10.1016/j.surfcoat.2016.10.076

[10] T.S. Sidhu, S. Prakash, R.D. Agrawal, Characterization of NiCr wire coatings on Ni- and Fe-based superalloys by the HVOF process, Surf. Coat. Technol. **200**, 5542-5549 (2006).
DOI: https://doi.org/10.1016/j.surfcoat.2005.07.101

[11] S. Tailor, A. Modi, S.C. Modi, High-Performance Molybdenum Coating by Wire-HVOF Thermal Spray Process, J. Therm. Spray Technol. **27**, 757-768 (2018).
DOI: https://doi.org/10.1007/s11666-018-0706-2.

[12] C. Senderowski, N. Cinca, S. Dosta, I.G. Cano, J.M. Guilemany, The Effect of Hot Treatment on Composition and Microstructure of HVOF Iron Aluminide Coatings in Na_2SO_4 Molten Salts. J Therm Spray Tech. **28**, 1492-1510 (2019). DOI: https://doi.org/10.1007/s11666-019-00886-w

[13] C. Senderowski, Z. Bojar, Gas detonation spray forming of Fe–Al coatings in the presence of interlayer. Surf. Coat. Technol. **202** (15), 3538-3548 (2008). DOI: https://doi.org/10.1016/j.surfcoat.2007.12.029

[14] E. Sadeghi, S. Joshi, Chlorine-induced high-temperature corrosion and erosion-corrosion of HVAF and HVOF-sprayed amorphous Fe-based coatings. Surf. Coat. Technol. **371**, 20-35 (2019). DOI: https://doi.org/10.1016/j.surfcoat.2019.01.080

[15] S.M. Muthu, M. Arivarasu, N. Arivazhagan, M.N. Rao, Investigation of hot corrosion resistance of bare and Ni-20%Cr coated superalloy 825 to Na2SO4-60%V2O5 environment at 900°C. Procedia Struct. Integr. **14**, 290-303 (2019). DOI: https://doi.org/10.1016/j.prostr.2019.05.037

[16] D. Pradhan, G.S. Mahobia, K. Chattopadhyay, V. Singh, Effect of surface roughness on corrosion behavior of the superalloy IN718 in simulated marine environment. J. Alloys Compd. **740**, 250-263 (2018). DOI: https://doi.org/10.1016/j.jallcom.2018.01.042

[17] N. Bala, H. Singh, S. Prakash, High-temperature oxidation studies of cold-sprayed Ni–20Cr and Ni–50Cr coatings on SAE 213-T22 boiler steel. Appl. Surf. Sci. **255** (15), 6862-6869 (2009). DOI: https://doi.org/10.1016/j.apsusc.2009.03.006

[18] C. Hempel, M. Mandel, C. Schimpf, L. Krüger, Long-term low-temperature hot corrosion of PTA welded René 41 superalloy under marine-like conditions. Mater. Corros. (April), (2022). DOI: https://doi.org/10.1002/maco.202213053

[19] S. Mohan Kumar, A. Rajesh Kannan, R. Pramod, N. Siva Shanmugam, S.M. Muthu, V. Dhinakaran, Microstructure and high temperature performance of 321 SS wall manufactured through wire + arc additive manufacturing. Mater. Lett. **314**, 131913 (2022). DOI: https://doi.org/10.1016/j.matlet.2022.131913

[20] D. Migas, M. Kierat, G. Moskal, The oxide scales formed on different Co-Ni based superalloys during isothermal oxidation at 800 and 900°C. Arch. Metall. and Mater. **66**, 5-14 (2021). DOI: https://doi.org/10.24425/amm.2021.134752

[21] V. Mannava, A.S. Rao, N. Paulose, M. Kamaraj, R.S. Kottada, Hot corrosion studies on Ni-base superalloy at 650°C under marine-like environment conditions using three salt mixture (Na_2SO_4+ NaCl+ $NaVO_3$). Corros. Sci. **105**, 109-119 (2016). DOI: https://doi.org/10.1016/j.corsci.2019.07.010

[22] G.S. Mahobia, N. Paulose, V. Singh, Hot Corrosion Behavior of Superalloy IN718 at 550 and 650°C. J. Mater. Eng. Perform. **22** (8), 2418-2435 (2013). DOI: https://doi.org/10.1007/s11665-013-0532-0

[23] W. Xie, X. Xing, Z. Cao, Thermodynamic, lattice dynamical, and elastic properties of iron-vanadium oxides from experiments and first principles. J. Am. Ceram. Soc. **103**, (2020). DOI: https://doi.org/10.1111/jace.17064

[24] R.A. Rapp, Hot corrosion of materials: a fluxing mechanism? Corros. Sci. **44** (2), 209-221 (2002). DOI: https://doi.org/10.1016/S0010-938X(01)00057-9

[25] M. Yu, T. Cui, D. Zhou, R. Li, J. Pu, C. Li, Improved oxidation and hot corrosion resistance of the NiSiAlY alloy at 750°C. Mater. Today Commun. **29**, 102939 (2021). DOI: https://doi.org/10.1016/j.mtcomm.2021.102939